

Anion- and Solvent-Directed Assembly in Silver Bis(thioimidazolyl)methane Chemistry and the Silver–Sulfur Interaction

Rosalice M. Silva,[†] Mark D. Smith,[‡] and James R. Gardinier^{*†}

Department of Chemistry, Marquette University, Milwaukee, Wisconsin 53201-1881, and Department of Chemistry and Biochemistry, University of South Carolina, Columbia, South Carolina 29208

Received November 23, 2005

The effect of metal complexation on the structure and properties of the electroactive bis(1-methylthioimidazolyl)methane linkage isomers $\text{CH}_2(\text{N-tim})_2$ (**L1**) and $\text{CH}_2(\text{S-tim})_2$ (**L2**) has been explored. Coordination polymers $\{[\text{Ag}(\text{L1})_2]\text{X}\}_n$ ($\text{X} = \text{BF}_4, \text{PF}_6$) are formed by bridging **L1** between tetrahedral silver centers giving two-dimensional cationic sheets composed of AgS_4 linkages; the anions are sandwiched between sheets. Cyclic dimers $\{[\text{Ag}_2(\text{L2})_2]\text{X}_2\}$ ($\text{X} = \text{BF}_4, \text{PF}_6, \text{OSO}_2\text{CF}_3$) are formed when **L2**: AgX ratios are lower than 1.5. When **L2**: AgPF_6 was 1.5 or higher, the complex $[\text{Ag}_4(\text{L2})_5](\text{PF}_6)_4$ could be isolated as a solvate. The NMR, IR, electrochemical, and ESI(+) mass spectral data of this latter compound indicate that extensive dissociation to the cyclic dimer and free ligand occurs in solution. Finally, a Cambridge Structural Database search was performed to provide insight into reasonable silver–sulfur bond distances, since literature values appeared to vary widely between 2.3 and 3.2 Å. It was found that these distances increase with increasing coordination number of silver. The average distances for 2-, 3-, 4-, 5-, and 6-coordinate silver were found to be 2.40, 2.52, 2.62, 2.70, and 2.75 Å, respectively.

Introduction

There has been a growing interest in the chemistry of multitopic ligands with “soft” Lewis donors for fundamental studies in the coordination and supramolecular chemistry of traditionally “soft” metals, as classified by Pearson.¹ In particular, systems designed to exploit the soft–soft interaction between silver(I) and sulfur-containing ligands² have been examined for studies in bioinorganic chemistry^{3a,b} and for their ability to assemble into diverse and aesthetically

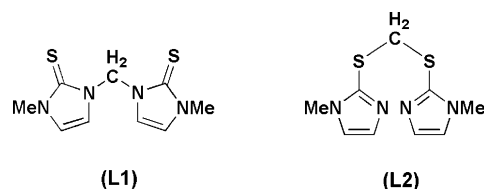


Figure 1. Two linkage isomers of the bis(thioimidazolyl)methane family of compounds: (left) CN isomer $\text{CH}_2(\text{N-tim})_2$ (**L1**); (right) CS isomer $\text{CH}_2(\text{S-tim})_2$ (**L2**).

pleasing coordination network architectures,^{3c} as well as for their ability to permit access to unusual oxidation states of silver.⁴ We have recently reported a (re)investigation into the synthesis and electrochemistry of the bis(thioimidazolyl)methane family of compounds (Figure 1).⁵ These compounds are attractive owing to both their potential biomedical applications⁶ and their potential utility in fundamental coordination chemistry.^{7–9} In the latter regard, it has been established that the reduction of imidazolinethiones with potassium metal provides one synthetic route to NCN

* To whom correspondence should be addressed. E-mail: james.gardinier@marquette.edu.

[†] Marquette University.

[‡] University of South Carolina.

- (1) Pearson, R. G. *J. Am. Chem. Soc.* **1963**, *85*, 3533. (b) R. G. Pearson, Ed. *Hard and Soft Acids and Bases*; Dowden, Hutchinson & Ross: Stroudsburg, PA, 1973.
- (2) See for example: (a) Han, L.; Wu, B.; Xu, Y.; Gong, Y.; Lou, B.; Chen, B.; Hong, M. *Inorg. Chim. Acta* **2005**, *358*, 2005. (b) Xie, Y.-B.; Zhang, C.; Li, J.-R.; Bu, X.-H. *Dalton Trans.* **2004**, 562. (c) Zheng, Y.; Du, M.; Li, J.-R.; Zhang, R.-H.; Bu, X.-H. *Dalton Trans.* **2003**, 1509.
- (3) (a) Parkin, G. *Chem. Rev.* **2004**, *104*, 699. (b) Vahrenkamp, H. *Acc. Chem. Res.* **1999**, *32*, 589. (c) Awaleh, M. O.; Badia, A.; Brisse, F. *Inorg. Chem.* **2005**, *44*, 7833. (d) Awaleh, M. O.; Badia, A.; Brisse, F. *Cryst. Growth Des.* **2005**, *5*, 1897. (e) Yoon, I.; Seo, J.; Lee, J.-E.; Song, M. R.; Lee, S. Y.; Choi, K. S.; Jung, O.-S.; Park, K.-M.; Lee, S. S. *Dalton Trans.* **2005**, 2352. (f) Tsuchiya, T.; Shimizu, T.; Hirabayashi, K.; Kamigata, N. *J. Org. Chem.* **2002**, *67*, 6632.

(4) Blake, A. J.; Coilson, D.; Gould, R. O.; Reid, G.; Schroder, M. *J. Chem. Soc., Dalton Trans.* **1993**, 521.

(5) Silva, R. M.; Smith, M. D.; Gardinier, J. R. *J. Org. Chem.* **2005**, *70*, 8755.

(6) (a) Roy, G.; Nethaji, M.; Mughesh, G. *J. Am. Chem. Soc.* **2004**, *126*, 2712. (b) Roy, G.; Mughesh, G. *J. Am. Chem. Soc.* **2005**, *127*, 15207.

carbenes.¹⁰ We initially examined the electrochemistry of these bis(thioimidazolyl)methanes by voltammetry in hope of finding a milder reducing agent for the generation of geminal polytopic carbenes, derived from compounds such as **L1**. Rather unexpectedly, we found that the CN isomer **L1** exhibited an irreversible two-electron oxidation centered near +0.7 V versus Ag/AgCl whereas the other linkage isomer **L2** exhibited two one-electron oxidations at +1.19 and +1.51 V where the first oxidation is irreversible and the second oxidation is quasi-reversible, reminiscent of an ECE reaction. The difference between the electrochemistry of these derivatives was attributed to the ability of the CS isomer (**L2**) to adopt a cofacial π -stacking geometry that would intramolecularly stabilize a one-electron oxidized intermediate species while such geometry is impossible for the CN-isomer (**L1**). We became interested in determining the effect of metal complexation on the electrochemistry of the ligands, with the goal of preparing new electroactive metal-organic framework materials and, possibly, to elucidate the nature of the electrochemistry of the ligands since attempts to characterize the direct oxidation products have not yet been fruitful. During the course of these studies, we have prepared and characterized several interesting silver complexes of these ligand systems and have identified a new binding mode for $\text{CH}_2(\text{S-tim})_2$ (**L2**) that we communicate in this report.

Experimental Section

The solvents used in the preparations were dried by conventional methods and distilled prior to use. The ligands $\text{CH}_2(\text{S-tim})_2$ and $\text{CH}_2(\text{N-tim})_2$ were prepared according to the recently published modification³ of the literature procedures.^{8,9} The uncomplexed silver salts were stored and handled under inert atmosphere; however, no special precautions were taken to avoid atmospheric moisture for the manipulation of the resulting complexes. Midwest MicroLab, LLC, Indianapolis, IN 45250, performed all elemental analyses. ¹H and ¹³C NMR spectra were recorded on a Varian 300 MHz spectrometer. Chemical shifts were referenced to solvent resonances at δ_{H} 2.05, δ_{C} 29.8 for acetone-*d*₆, δ_{H} 1.94, δ_{C} 118.9 for CD₃CN, and δ_{H} 2.50, δ_{C} 39.51 for DMSO. Melting point determinations were made on samples contained in glass capillaries using an Electrothermal 9100 apparatus and are uncorrected. Electrochemical measurements were collected with a BAS CV-50V instrument at a scan rate of 200 mV/s using CH₃CN solutions that were 0.1–0.8 mM in silver complex, 0.1 M of either NBu₄BF₄, NBu₄OTf, or NBu₄PF₆ as the supporting electrolyte, in a three-electrode cell comprised of a Ag/AgCl electrode, a platinum working electrode, and a glassy carbon counter electrode.

While most other characterization data for the $\text{CH}_2(\text{tim})_2$ ligands can be found elsewhere,^{5,9,10} the following missing data are reported for reference:

CH₂(N-tim)₂: ¹H NMR (acetone-*d*₆) δ_{H} 7.51 (d, *J* = 2 Hz, 2H, tim), 6.98 (d, *J* = 2 Hz, 2H, tim), 6.25 (s, 2H, CH₂), 3.53 (s, 6H, NCH₃); ¹³C NMR (acetone-*d*₆) δ_{C} SCN₂ not obsd (C=S), 118.8 (=CH), 118.4 (=CH), 56.7 (CH₂), 35.0 (NCH₃); ¹H NMR (CD₃CN) δ_{H} 7.44 (d, *J* = 2 Hz, 2H, tim), 6.79 (d, *J* = 2 Hz, 2H, tim), 6.19 (s, 2H, CH₂), 3.48 (s, 6H, NCH₃); ¹³C NMR (CD₃CN) δ_{C} SCN₂ not obsd, 119.8 (=CH), 119.2 (=CH), 57.7 (CH₂), 35.9 (NCH₃); IR (KBr, cm⁻¹) 3165, 3127, 3098, 2972, 2943, 1654, 1570, 1461, 1440, 1389, 1373, 1328, 1296, 1266, 1230, 1208, 1162, 1093, 969, 823, 795, 770, 711, 683, 675, 524.

CH₂(S-tim)₂: ¹H NMR (acetone-*d*₆) δ_{H} 7.14 (d, *J* = 1 Hz, 2H, tim), 6.97 (d, *J* = 1 Hz, 2H, tim), 4.69 (s, 2H, CH₂), 3.61 (s, 6H, NCH₃); ¹³C NMR (acetone-*d*₆) δ_{C} 155.1 (C=S), 129.1 (=CH), 123.1 (=CH), 39.1 (CH₂), 32.5 (NCH₃); ¹H NMR (CD₃CN) δ_{H} 7.06 (d, *J* = 1 Hz, 2H, tim), 6.98 (d, *J* = 1 Hz, 2H, tim), 4.57 (s, 2H, CH₂), 3.56 (s, 6H, NCH₃); ¹³C NMR (CD₃CN) δ_{C} 141.1 (SCN₂), 130.6 (=CH), 125.0 (=CH), 41.1 (CH₂), 34.4 (NCH₃); IR (KBr, cm⁻¹) 3175, 3133, 3093, 3004, 2939, 1683, 1510, 1458, 1412, 1378, 1337, 1280, 1209, 1126, 1082, 922, 830, 753, 686.

General Procedures for the Syntheses of Silver Complexes.

Method A. A 10 mL THF solution containing approximately 0.2–2.0 mmol (as below) of the desired ligand [gentle heating is required to dissolve $\text{CH}_2(\text{N-tim})_2$] is added by cannula to a 10 mL THF solution of the desired ligand. The flask that originally contained the ligand is washed with an additional 5 mL of THF to ensure quantitative transfer to the reaction mixture. The desired complex typically begins precipitating within a few minutes of mixing. The mixture is stirred 4 h at room temperature and filtered. The solid product is washed with 5 mL of THF and two 10 mL portions of Et₂O and dried under vacuum.

Method B. The procedure is essentially the same as above, but the reaction mixture is heated at reflux 4 h rather than being maintained at room temperature. Further, the solid residue is then dissolved in CH₃CN, the resulting solution passed through a plug of Celite. The complex is precipitated by the addition of copious Et₂O, and it is isolated after filtration and drying under vacuum.

Bis[S,S-bis(2-thione-3-methylimidazolyl)methane]silver(I) Tetrafluoroborate, [Ag(L1)₂](BF₄). Method A. The reaction between 0.20 g (0.832 mmol) of $\text{CH}_2(\text{N-tim})_2$ and 0.081 g (0.42 mmol) of AgBF₄ afforded 0.25 g (90%) of [Ag(L1)₂](BF₄) as a colorless powder. Mp: 230 °C (dec). Anal. Calcd (found) for C₁₈H₂₄AgBF₄N₈S₄: C, 32.01 (31.79); H, 3.58 (3.70); N, 16.59 (16.40). IR (KBr, cm⁻¹): 3174, 3146, 3116, 3029, 2942, 1570, 1467, 1426, 1395, 1348, 1326, 1307, 1245, 1229, 1220, 1209, 1155, 1100–1000 br, 954, 789, 770, 758, 727, 694, 673, 657, 650, 513. ¹H NMR (acetone-*d*₆): δ_{H} 7.52 (d, *J* = 2 Hz, 2H, tim), 7.34 (d, *J* = 2 Hz, 2H, tim), 6.58 (s, 2H, CH₂), 3.60 (s, 6H, CH₃). ¹³C NMR (δ , acetone-*d*₆): δ_{H} 159.1 (SCN₂), 121.8 (tim), 119.3 (tim), 58.3 (CH₂), 36.2 (NCH₃). ¹H NMR (CD₃CN): δ_{H} 7.18 (d, *J* = 2 Hz, 2H, tim), 7.00 (d, *J* = 2 Hz, 2H, tim), 6.30 (s, 2H, CH₂), 3.47 (s, 6H, NCH₃). ¹³C NMR (CD₃CN): δ_{C} 159.3 (C=S), 120.7 (=CH), 118.3 (=CH), 57.6 (CH₂), 35.5 (NCH₃). HRMS [ESI(+), *m/z*] {calcd (obsd) for C₁₈H₂₄Ag₂N₈S₄, [AgL₂⁺]}: 587.0058 (587.0052). ESI(+) MS (CH₃CN) {*m/z* (int) [assign]}: 589 (60) [AgL₂⁺], 389 (10) [AgL(CH₃CN)⁺], 349 (100) [AgL⁺]. Single crystals for X-ray diffraction were grown by vapor diffusion of Et₂O into CH₃CN solutions of the complex.

Method B. A mixture of 0.042 g (0.21 mmol) of AgBF₄ and 0.100 g (0.42 mmol) of $\text{CH}_2(\text{N-tim})_2$ afforded 0.096 g (68% yield)

- (7) (a) Bigoli, F.; Deplano, P.; Devillanova, F. A.; Lippolis, V.; Mercuri, M. L.; Pellinghelli, M. A.; Trogu, E. F. *Inorg. Chim. Acta* **1998**, *267*, 115. (b) Bigoli, F.; Deplano, P.; Mercuri, M. L.; Pellinghelli, M. A.; Sabatini, A.; Trogu, E. F.; Vacca, A. *J. Chem. Soc., Dalton Trans.* **1996**, 3583. (c) Williams, D. J.; Shilatifard, A.; VanDerveer, D.; Lipscomb, L. A.; Jones, R. L. *Inorg. Chim. Acta* **1992**, *202*, 53.
 (8) (a) Williams, D. J.; VanDerveer, D.; Jones, R. L.; Menaldino, D. S. *Inorg. Chim. Acta* **1989**, *165*, 173. (b) Bark, L. S.; Chadwick, N.; Meth-Cohn, O. *Tetrahedron* **1992**, *48*, 7863.
 (9) Casas, J. S.; Castiñeiras, A.; García Martínez, E.; Rodríguez Rodríguez, P.; Russo, U.; Sánchez, A.; Sánchez González, A.; Sordo, J. *Appl. Organomet. Chem.* **1999**, *13*, 69.
 (10) Kuhn, N.; Kratz, T. *Synthesis* **1993**, 561.

of $[\text{Ag}(\text{L1})_2](\text{BF}_4)$ whose characterization data matched those from the previous preparation.

$[\text{N},\text{N}$ -Bis(1-methyl-1*H*-imidazol-2-ylthio)methane]silver(I) Tetrafluoroborate, $[\text{Ag}(\text{L2})](\text{BF}_4)$. Method A. A mixture of 0.244 g of $\text{CH}_2(\text{S-tim})_2$ (1.02 mmol) and 0.198 g (1.02 mmol) of AgBF_4 afforded 0.405 g (92%) of pure $[\text{Ag}(\text{L2})](\text{BF}_4)$ as a colorless solid. Mp: 175 °C (dec). Anal. Calcd (found) for $\text{C}_{18}\text{H}_{24}\text{Ag}_2\text{B}_2\text{F}_8\text{N}_8\text{S}_4$: C, 24.84 (24.79); H, 2.78 (2.82); N 12.88 (12.79). IR (KBr, cm^{-1}): 3174, 3146, 3116, 3029, 2942, 1532, 1471, 1415, 1384, 1353, 1340, 1285, 1215, 1158, 1090 br, 1058 br, 1037 br, 955, 819, 759, 710, 693, 521. ^1H NMR (acetone- d_6): δ_{H} 7.55 (d, $J = 1$ Hz, 2H, tim), 7.15 (d, $J = 1$ Hz, 2H, tim), 4.61 (s, 2H, CH_2), 3.90 (s, 6H, NCH_3). ^{13}C NMR (acetone- d_6): δ_{C} 159.1 (C=S), 130.5 (=CH), 126.2 (=CH), 42.2 (CH_2), 34.8 (NCH_3). ^1H NMR (CD_3CN): δ_{H} , 7.33 (d, $J = 1$ Hz, 2H, tim), 7.05 (d, $J = 1$ Hz, 2H, tim), 4.16 (s, 2H, CH_2), 3.76 (s, 6H, NCH_3). ^{13}C NMR (CD_3CN): δ_{C} 139.8 (SCN_2), 131.3 (=CH), 127.1 (=CH), 43.5 (CH_2), 36.1 (CH_3). ESI(+) MS (CH_3CN) $\{m/z$ (int) [assign]}: 783 (2) $[\text{Ag}_2\text{L}_2 + \text{BF}_4]$, 589 (23) $[\text{AgL}_2^+]$, 389 (6) $[\text{AgL}(\text{CH}_3\text{CN})^+]$, 349 (100) $[\text{AgL}^+]$, 241 (29) $[\text{HL}^+]$, 189 (75) $[\text{Ag}(\text{CH}_3\text{CN})_2^+]$, 148 (19) $[\text{Ag}(\text{CH}_3\text{CN})^+]$, 128 (34) $[\text{CH}_2(\text{S-tim})^+]$, 114 (44) $[\text{H}_2(\text{stim})]$.

Method B. The reaction between 0.185 g (0.917 mmol) of AgBF_4 and 0.500 g (2.08 mmol) of $\text{CH}_2(\text{S-tim})_2$ afforded 0.398 g (98% yield based on AgBF_4) of $[\text{Ag}(\text{L2})](\text{BF}_4)$ as a colorless solid whose characterization data matched those from the previous preparation.

Bis[S,S-bis(2-thione-3-methylimidazolyl)methane]silver(I) Hexafluorophosphate, $[\text{Ag}(\text{L1})_2](\text{PF}_6)$ Method A. The reaction between 0.200 g (0.832 mmol) of $\text{CH}_2(\text{N-tim})_2$ and 0.105 g (0.416 mmol) of AgPF_6 afforded 0.325 g (97%) of $[\text{Ag}(\text{L1})_2](\text{PF}_6)\cdot\text{THF}$ as a colorless powder. Mp: 212 °C (dec). Anal. Calcd (found) for $\text{C}_{18}\text{H}_{26}\text{AgF}_6\text{O}_8\text{N}_8\text{PS}_4$: C, 28.77 (28.80); H, 3.49 (3.27); N, 14.91 (14.54). IR (KBr, cm^{-1}): 3178, 3147, 3120, 3029, 2942, 1571, 1464, 1425, 1396, 1376, 1340, 1308, 1304, 1245, 1228, 1209, 1155, 1085, 1067 br, 966, 855 br, 789, 758, 728, 697, 673, 658, 649, 559, 512. ^1H NMR (acetone- d_6): δ_{H} 7.52 (d, $J = 2$ Hz, 2H, tim), 7.33 (d, $J = 2$ Hz, 2H, tim), 6.58 (s, 2H, CH_2), 3.62 (m, OCH_2), 3.59 (s, 6H, NCH_3), 1.79 (m, thf- CH_2). ^{13}C NMR (acetone- d_6): δ_{C} 158.6 (C=S), 121.9 (=CH), 119.5 (=CH), 58.3 (CH_2), 36.3 (NCH_3). ^1H NMR (CD_3CN): δ_{H} 7.16 (d, $J = 2$ Hz, 2H, tim), 7.01 (d, $J = 2$ Hz, 2H, tim), 6.31 (s, 2H, CH_2), 3.49 (s, 6H, CH_3). ^{13}C NMR (CD_3CN): δ_{C} (NCS not obsd), 122.1 (=CH), 119.6 (=CH), 58.9 (CH_2), 36.7 (NCH_3). HRMS [ESI(+), m/z] {calcd (obsd) for $\text{C}_{18}\text{H}_{24}\text{Ag}_2\text{N}_8\text{S}_4$, $[\text{AgL}_2^+]$ }: 587.0058 (587.0066). ESI(+) MS (CH_3CN) $\{m/z$ (int) [assign]}: 2309 (0.2) $[\text{Ag}_4\text{L}_6(\text{PF}_6)_3^+]$, 2063 (0.3) $[\text{Ag}_4\text{L}_5(\text{PF}_6)_3^+]$, 1575 (2) $[\text{Ag}_3\text{L}_4(\text{PF}_6)_2^+]$, 1331 (1) $[\text{Ag}_3\text{L}_3(\text{PF}_6)_2^+]$, 1081 (4) $[\text{Ag}_2\text{L}_3(\text{PF}_6)^+]$, 841 (52) $[\text{Ag}_2\text{L}_2(\text{PF}_6)^+]$, 589 (90) $[\text{AgL}_2^+]$, 389 (25) $[\text{AgL}(\text{CH}_3\text{CN})^+]$, 349 (100) $[\text{AgL}^+]$. Single crystals suitable for X-ray diffraction were grown by vapor diffusion of Et_2O into a CH_3CN solution of the complex.

Method B. A mixture of 0.100 g (0.396 mmol) of AgPF_6 and 0.190 g (0.791 mmol) of $\text{CH}_2(\text{N-tim})_2$ afforded 0.141 g (72%) of $[\text{Ag}(\text{L1})_2](\text{PF}_6)$ as a colorless powder whose characterization data matched those from the previous preparation.

$[\text{N},\text{N}$ -Bis(1-methyl-1*H*-imidazol-2-ylthio)methane]silver(I) Hexafluorophosphate, $[\text{Ag}(\text{L2})](\text{PF}_6)$ Method A. A mixture of 0.233 g (0.969 mmol) of $\text{CH}_2(\text{S-tim})_2$ and 0.245 g (0.969 mmol) of AgPF_6 afforded 0.454 g (95%) of $[\text{Ag}(\text{L2})](\text{PF}_6)$ as a colorless solid. Mp: 182 °C (dec). Anal. Calcd (found) for $\text{C}_9\text{H}_{12}\text{AgF}_6\text{N}_4\text{PS}_2$: C, 21.92 (21.84); H, 2.45 (2.23); N, 11.36 (11.49). IR (KBr, cm^{-1}): 3146, 2958, 2871, 1521, 1462, 1414, 1384, 1357, 1330, 1283, 1214, 1140, 1138, 1085, 1060, 1025, 925, 877, 836, 771, 760, 692, 558. ^1H NMR (acetone- d_6): δ_{H} 7.59 (d, $J = 1$ Hz, 2H,

tim), 7.21 (d, $J = 1$ Hz, 2H, tim), 4.73 (s, 2H, CH_2), 3.91 (s, 6H, NCH_3). ^{13}C NMR (acetone- d_6): δ_{C} SCN_2 not obsd, 131.3 (=CH), 127.3 (=CH), 43.5 (CH_2), 35.6 (NCH_3). ^1H NMR (CD_3CN): δ_{H} 7.33 (d, $J = 1$ Hz, 2H, tim), 7.06 (d, $J = 1$ Hz, 2H, tim), 4.15 (s, 2H, CH_2), 3.77 (s, 6H, NCH_3). ^{13}C NMR (CD_3CN): δ_{C} 140.0 ($\text{N}_2\text{-CS}$), 131.5 (=CH), 127.2 (=CH), 43.2 (CH_2), 36.0 (NCH_3). HRMS [ESI(+), m/z] {calcd (obsd) for $\text{C}_{18}\text{H}_{24}\text{Ag}_2\text{N}_8\text{PS}_4$, $[\text{Ag}_2\text{L}_2 + \text{PF}_6]$ }: 840.8745 (840.8750). ESI(+) MS (CH_3CN) $\{m/z$ (int) [assign]}: 841 (13) $[\text{Ag}_2\text{L}_2 + \text{PF}_6]$, 589 (27) $[\text{AgL}_2^+]$, 389 (9) $[\text{AgL}(\text{CH}_3\text{CN})^+]$, 349 (100) $[\text{AgL}^+]$, 241 (40) $[\text{HL}^+]$, 189 (92) $[\text{Ag}(\text{CH}_3\text{CN})_2^+]$, 148 (20) $[\text{Ag}(\text{CH}_3\text{CN})^+]$, 128 (43) $[\text{CH}_2(\text{S-tim})^+]$, 114 (56) $[\text{H}_2(\text{stim})]$. Single crystals suitable for X-ray diffraction were grown by vapor diffusion of Et_2O into an acetone solution of the complex.

Pentakis[$[\text{N},\text{N}$ -bis(1-methyl-1*H*-imidazol-2-ylthio)methane]tetrasilver(I) Tetrakis(hexafluorophosphate), $[(\text{L2})_5\text{Ag}_4](\text{PF}_6)_4$. Method A. A mixture of 0.100 g (0.396 mmol) of AgPF_6 and 0.190 g (0.782 mmol) of $\text{CH}_2(\text{S-tim})_2$ afforded 0.136 g (61% based on AgPF_6) of $[\text{Ag}_4(\text{L2})_5](\text{PF}_6)_4\cdot\text{CH}_3\text{CN}$. Mp: 171 °C (dec). Anal. Calcd (found) for $\text{C}_{47}\text{H}_{63}\text{Ag}_4\text{F}_{24}\text{N}_{21}\text{P}_4\text{S}_{10}$: C, 25.04 (25.38); H, 2.79 (2.84); N, 13.05 (12.86). IR (KBr, cm^{-1}): 3130, 3100, 3025, 2940, 1520, 1463, 1413, 1384, 1358, 1337, 1283, 1214, 1145, 1085, 1020, 941, 879, 839 br, 771, 760, 688 625, 558, 520. ^1H NMR (CD_3CN): δ_{H} 7.32 (d, $J = 1$ Hz, 2H, tim), 7.04 (d, $J = 1$ Hz, 2H, tim), 4.19 (s, 2H, CH_2), 3.75 (s, 6H, CH_3). ^{13}C NMR (CD_3CN): δ_{C} 139.9 (N_2CS), 131.4 (=CH), 127.1 (=CH), 43.3 (CH_2), 35.9 (CH_3). Crystals of $[(\text{L2})_5\text{Ag}_4](\text{PF}_6)_4\cdot\text{CH}_3\text{CN}$ are formed along with crystals of $[\text{Ag}_2(\text{L2})_2](\text{PF}_6)_2$ after vapor diffusion of Et_2O into an acetonitrile solution of so-formed $[\text{Ag}_4(\text{L2})_5](\text{PF}_6)_4\cdot\text{CH}_3\text{CN}$ powder, as described later in the text.

Method B Attempt. A mixture of 0.100 g (0.396 mmol) of AgPF_6 and 0.118 g (0.495 mmol) of $\text{CH}_2(\text{S-tim})_2$ afforded 0.147 g of a colorless powder that analyzed as $[\text{Ag}(\text{L2})](\text{PF}_6)\cdot 3/8\text{THF}$ (69% based on AgPF_6). Anal. Calcd (found) for $\text{C}_{10.5}\text{H}_{15}\text{AgF}_6\text{N}_4\text{PO}_{0.385}\text{S}_2$: C, 23.43 (23.67); H, 2.81 (2.80); N, 10.41 (10.21).

Isolation of $[\text{Ag}(\text{L2})](\text{PF}_6)\cdot\text{THF}$ from Attempted Preparation of Tetrakis[bis(1-methyl-1*H*-imidazol-2-ylthio)methane]trisilver(I) Hexafluorophosphate, $[(\text{L2})_4\text{Ag}_3](\text{PF}_6)_3$. Method A. A mixture of 0.188 g (0.782 mmol) of $\text{CH}_2(\text{S-tim})_2$ and 0.148 g (0.585 mmol) of AgPF_6 afforded 0.255 g (77%) of $[\text{Ag}(\text{L2})](\text{PF}_6)\cdot\text{THF}$ as a colorless solid. Anal. Calcd (found) for $\text{C}_{13}\text{H}_{20}\text{AgF}_6\text{N}_4\text{OPS}_2$: C, 27.62 (27.61); H, 3.57 (3.60); N, 9.91 (10.03). IR (KBr, cm^{-1}): ^1H NMR (acetone- d_6): δ_{H} 7.59 (d, $J = 1$ Hz, 2H, tim), 7.20 (d, $J = 1$ Hz, 2H, tim), 4.70 (s, 2H, CH_2), 3.91 (s, 6H, NCH_3), 3.62 (THF, OCH_2), 1.78 (THF, CCH_2). ^{13}C NMR (acetone- d_6): δ_{C} $\text{N}_2\text{-CS}$ not obsd, 130.7 (=CH), 126.6 (=CH), 68.1 (THF), 42.8 (CH_2), 34.9 (NCH_3), 26.1 (THF). ESI(+) MS (CH_3CN) $\{m/z$ (int) [assign]}: 841 (41) $[\text{Ag}_2\text{L}_2(\text{PF}_6)^+]$, 349 (100) $[\text{AgL}^+]$, 241 (90) $[\text{HL}^+]$. Trace peaks (in baseline of high m/z): 2321 (10) $[\text{Ag}_5\text{L}_5(\text{PF}_6)_4^+]$, 1827 (29) $[\text{Ag}_4\text{L}_4(\text{PF}_6)_3^+]$, 1575 (5) $[\text{Ag}_3\text{L}_4(\text{PF}_6)_2^+]$, 1335 (100) $[\text{Ag}_3\text{L}_3(\text{PF}_6)_2^+]$.

Bis[S,S-bis(2-thione-3-methylimidazolyl)methane]silver(I) Triflate, $[\text{Ag}(\text{L1})_2](\text{OTf})$. Method A. The reaction mixture of 0.200 g (0.832 mmol) of $\text{CH}_2(\text{N-tim})_2$ and 0.107 g (0.416 mmol) of AgOTf was initially very slow to precipitate (20 min) but after stirring overnight afforded 0.286 g [93% yield based on $\text{Ag}(\text{OTf})$] of $[\text{Ag}(\text{L1})_2](\text{OTf})\cdot 1/2\text{THF}$ as a colorless solid. Mp: 141 °C (dec). Anal. Calcd (found) for $\text{C}_{21}\text{H}_{28}\text{AgF}_3\text{N}_8\text{O}_{3.5}\text{S}_5$: C, 32.60 (32.54); H, 3.65 (3.63); N, 14.48 (13.92). IR (KBr, cm^{-1}): 3168, 3127, 2945, 1573, 1473, 1462, 1425, 1397, 1387, 1376, 1340, 1312, 1280, 1260, 1227, 1210, 1160, 1156, 1092, 1069 br, 1031, 966, 781, 760, 723, 705, 668, 650, 573, 518. ^1H NMR (acetone- d_6): δ_{H} 7.56 (d, $J = 2$ Hz, 2H, tim), 7.37 (d, $J = 2$ Hz, 2H, tim), 6.60 (s, 2H, CH_2), 3.62 (s, 3H, NCH_3). ^{13}C NMR (acetone- d_6): δ_{C} 158.6 (C=S), 121.9

Table 1. Crystallographic Data and Refinement Parameters for [Ag(L1)₂](BF₄) (I), [Ag(L1)₂](PF₆) (II), [Ag₂(L2)₂](BF₄)₂ (III), [Ag₂(L2)₂](PF₆)₂·2C₃H₆O (IV), [Ag₄(L2)₅](PF₆)₄·CH₃CN (V), and [Ag₂(L2)₂](SO₃CF₃)₂ (VI)

param	I	II	III	IV	V	VI
formula	C ₁₈ H ₂₄ AgBF ₄ N ₈ S ₄	C ₁₈ H ₂₄ AgF ₆ N ₈ PS ₄	C ₁₈ H ₂₄ Ag ₂ B ₂ F ₈ N ₈ S ₄	C ₂₄ H ₃₆ Ag ₂ F ₁₂ N ₈ O ₂ P ₂ S ₄	C ₄₇ H ₆₃ Ag ₄ F ₂₄ N ₂₁ P ₄ S ₁₀	C ₂₀ H ₂₄ Ag ₂ F ₆ N ₈ O ₆ S ₆
fw	675.37	733.53	870.05	1102.53	2254.14	994.57
cryst system	monoclinic	monoclinic	orthorhombic	triclinic	monoclinic	orthorhombic
space group	<i>P</i> 2 ₁ / <i>c</i>	<i>P</i> 2 ₁ / <i>c</i>	<i>Pca</i> 2 ₁	<i>P</i> $\bar{1}$	<i>P</i> 2 ₁ / <i>n</i>	<i>Pbca</i>
<i>a</i> , Å	10.5310(6)	10.3342(7)	12.5631(6)	12.2593(8)	14.3275(6)	12.8641(7)
<i>b</i> , Å	14.1350(8)	14.2812(9)	10.9887(5)	12.3743(8)	24.8141(11)	22.0250(12)
<i>c</i> , Å	18.2045(10)	18.9471(13)	21.2710(9)	15.2717(9)	22.6936(10)	23.7696(13)
α , deg	90	90	90	106.1110(10)	90	90
β , deg	103.6290(10)	101.8000(10)	90	93.4160(10)	102.8110(10)	90
γ , deg	90	90	90	115.3340(10)	90	90
<i>V</i> , Å ³	2633.5(3)	2737.2(3)	2936.5(2)	1968.8(2)	7867.3(6)	6734.7(6)
<i>Z</i>	4	4	4	2	4	8
<i>T</i> , K	150(1)	150(1)	150(1)	150(1)	150(1)	150(1)
ρ_{calcd} , Mg m ⁻³	1.703	1.780	1.968	1.860	1.903	1.962
λ , Å	0.710 73	0.710 73	0.710 73	0.710 73	0.710 73	0.710 73
$\mu(\text{Mo K}\alpha)$, mm ⁻¹	1.136	1.167	1.696	1.382	1.435	1.618
<i>R</i> [<i>I</i> > 2 σ (<i>I</i>)] ^a (all data)	0.0321 (0.0392)	0.0291 (0.0351)	0.0310 (0.0325)	0.0294 (0.0320)	0.0367 (0.0597)	0.0391 (0.0444)
w <i>R</i> ^b (all data)	0.0760 (0.0784)	0.0649 (0.0667)	0.0777 (0.0788)	0.0759 (0.0773)	0.0668 (0.0729)	0.0973 (0.1005)

$$^a R = \sum |F_o| - \sum |F_c| / \sum |F_o|, ^b wR = [\sum w(|F_o|^2 - |F_c|^2)^2 / \sum w|F_o|^2]^{1/2}.$$

(=CH), 119.5 (=CH), 58.3 (CH₂), 36.3 (NCH₃). ¹H NMR (CD₃-CN): δ_{H} 7.15 (d, *J* = 2 Hz, 2H, tim), 7.08 (d, *J* = 2 Hz, 2H, tim), 6.33 (s, 2H, CH₂), 3.52 (s, 3H, NCH₃). ¹³C NMR (CD₃CN): δ_{C} 160.7 (C=S), 122.0 (=CH), 119.6 (=CH), 58.8 (CH₂), 36.7 (NCH₃). HRMS [ESI(+), *m/z*] {calcd (obsd) for C₁₈H₂₄Ag₂N₈S₄, [AgL₂⁺]}: 587.0058 (587.0051). ESI(+)-MS (CH₃CN) {*m/z* (int) [assign]}: 2081 (1) [Ag₄L₅(OTf)₃⁺], 1841 (0.5) [Ag₄L₄(OTf)₃⁺], 1583 (3) [Ag₃L₄(OTf)₂⁺], 1343 (5) [Ag₃L₃(OTf)₂⁺], 1085 (1) [Ag₂L₃(OTf)⁺], 845 (64) [Ag₂L₂(OTf)⁺], 589 (90) [AgL₂⁺], 389 (28) [AgL(CH₃CN)⁺], 349 (100) [AgL⁺].

[S,S-Bis(2-thione-3-methylimidazolyl)methane]silver(I) Tri-flate, [Ag(L1)](OTf). Method B. The reaction between 0.214 g (0.832 mmol) of AgOTf and 0.200 g (0.832 mmol) of CH₂(N-tim)₂ afforded 0.210 g (51%) of [Ag(L1)](OTf) as a colorless solid. Mp: 192 °C (dec). Anal. Calcd (found) for C₂₀H₂₄Ag₂F₆N₈O₆S₆: C, 24.15 (24.19); H, 2.43 (2.45); N 11.26 (11.22). IR (KBr, cm⁻¹): 3173, 3136, 3108, 3015, 1580, 1472, 1462, 1415, 1400, 1385, 1373, 1322, 1283, 1251, 1240, 1224, 1215, 1168, 1158, 1137, 1098, 1067 br, 1029, 979, 794, 765, 758, 729, 700, 663, 638, 574, 517. ¹H NMR (acetone-*d*₆): δ_{H} 7.26 (d), 7.17 (d, *J* = Hz), 6.60 (CH₂), 3.62 (NCH₃). ¹³C NMR (acetone-*d*₆): δ_{C} 158.6 (C=S), 121.9 (=CH), 119.5 (=CH), 58.3 (CH₂), 36.3 (NCH₃). ¹H NMR (CD₃CN): δ_{H} 7.23 (d, *J* = 1 Hz, 2H, tim), 7.17 (d, *J* = 1 Hz, 2H, tim), 6.35 (s, 2H, CH₂), 3.60 (s, 6H, NCH₃). ¹³C NMR (CD₃CN): δ_{C} N₂CS not obsd, 123.2 (=CH), 120.5 (=CH), 59.3 (CH₂), 37.3 (CH₃). HRMS [ESI(+), *m/z*] {calcd (obsd) for C₉H₁₂AgN₄S₂, [AgL⁺]}: 346.9554 (346.9556). ESI(+)-MS (CH₃CN) {*m/z* (int) [assign]}: 1343 (15) [Ag₃L₃(OTf)₂⁺], 845 (100) [Ag₂L₂(OTf)⁺], 589 (33) [AgL₂⁺], 389 (23) [AgL(CH₃CN)⁺], 349 (100) [AgL⁺], 241 (13) [HL⁺].

[N,N-Bis(1-methyl-1H-imidazol-2-ylthio)methane]silver(I) Tri-flate, [Ag(L2)](OTf). Method A. A mixture of 0.229 g (0.953 mmol) of CH₂(S-tim)₂ and 0.245 g (0.953 mmol) of Ag(OTf) afforded 0.400 g (84% yield) of pure [Ag(L2)](OTf) as a colorless powder. Mp: 152 °C (dec). Anal. Calcd (found) for C₂₀H₂₄-Ag₂F₆N₈O₆S₆: C, 24.15 (23.94); H, 2.43 (2.49); N 11.26 (10.48). IR (KBr, cm⁻¹): 3127, 3000, 2958, 1522, 1464, 1414, 1384, 1345, 1280, 1263, 1225, 1212, 1159, 1140, 1080, 1045, 1030, 966, 757, 693, 638, 573, 518. ¹H NMR (acetone-*d*₆): δ_{H} 7.59 (d, *J* = 1 Hz, 2H, tim), 7.23 (d, *J* = 1 Hz, 2H, tim), 4.73 (s, 2H, CH₂), 3.91 (s, 6H, NCH₃). ¹³C NMR (acetone-*d*₆): δ_{C} 139.8 (SCN₂), 131.3 (=CH), 127.1 (=CH), 43.5 (CH₂), 35.5 (NCH₃). ¹H NMR (CD₃CN): δ_{H} 7.36 (d, *J* = 1 Hz, 2H, tim), 7.08 (d, *J* = 1 Hz, 2H, tim), 4.21 (s, 2H, CH₂), 3.76 (s, 6H, NCH₃). ¹³C NMR (CD₃CN): δ_{C} 139.9

(N₂CS), 131.4 (=CH), 127.3 (=CH), 43.9 (CH₂), 36.3 (CH₃). HRMS [ESI(+), *m/z*] {calcd (obsd) for C₁₉H₂₄Ag₂N₈O₃S₅, [Ag₂L₂ + OTf]}: 844.8622 (844.8630). ESI(+)-MS (CH₃CN) {*m/z* (int) [assign]}: 845 (13) [Ag₂L₂ + OTf], 589 (5) [AgL₂⁺], 388 (6) [AgL(CH₃CN)⁺], 349 (100) [AgL⁺], 189 (36) [Ag(CH₃CN)₂⁺], 148 (10) [Ag(CH₃CN)⁺].

Method B. A mixture of 0.213 g (0.832 mmol) of AgOTf and 0.200 g (0.832 mmol) of CH₂(S-tim)₂ afforded 0.252 g (72%) of [Ag(L2)](OTf) as a colorless powder.

Crystallography. General Considerations. X-ray intensity data from a colorless plate of [Ag(L1)₂](BF₄) (I), a colorless blocklike crystal of [Ag(L1)₂](PF₆) (II), a colorless plate of [Ag₂(L2)₂](BF₄)₂ (III), a colorless prism of [Ag₂(L2)₂](PF₆)₂·2C₃H₆O (IV), a colorless block of [Ag₄(L2)₅](PF₆)₄·CH₃CN (V), and a colorless needle of [Ag₂(L2)₂](SO₃CF₃)₂ (VI) were measured at 150(1) K on a Bruker SMART APEX CCD-based diffractometer (Mo K α radiation, λ = 0.710 73 Å).¹¹ Raw data frame integration and *Lp* corrections were performed with SAINT+.¹¹ Final unit cell parameters were determined by least-squares refinement of 6287 reflections for I, 5137 reflections for II, 9744 reflections for III, 8028 reflections for IV, 6415 reflections for V, and 9623 reflections for VI each with *I* > 5 σ (*I*) from their respective data sets (Table 1). For each, analysis of the data showed negligible crystal decay during collection. The data for [Ag₂(L2)₂](BF₄)₂ (III) were corrected for absorption effects with SADABS.¹¹ Direct methods structure solutions, difference Fourier calculations, and full-matrix least-squares refinements against *F*² were performed with SHELXTL.¹² All non-hydrogen atoms were refined with anisotropic displacement parameters except where noted below. Hydrogen atoms were placed in geometrically idealized positions and included as riding atoms.

Details. The compound [Ag(L1)₂](BF₄) (I) crystallizes in the space group *P*2₁/*c* as determined uniquely by the pattern of systematic absences in the intensity data. The asymmetric unit contains one Ag atom, two independent C₉H₁₂N₄S₂ ligands, and a BF₄⁻ anion.

The compound [Ag(L1)₂](PF₆) (II) crystallizes in the space group *P*2₁/*c* as determined uniquely by the pattern of systematic absences in the intensity data. The asymmetric unit consists of one formula unit.

(11) SMART Version 5.625, SAINT+ Version 6.22, and SADABS Version 2.05; Bruker Analytical X-ray Systems, Inc.: Madison, WI, 2001.

(12) Sheldrick, G. M. SHELXTL Version 6.1; Bruker Analytical X-ray Systems, Inc.: Madison, WI, 2000.

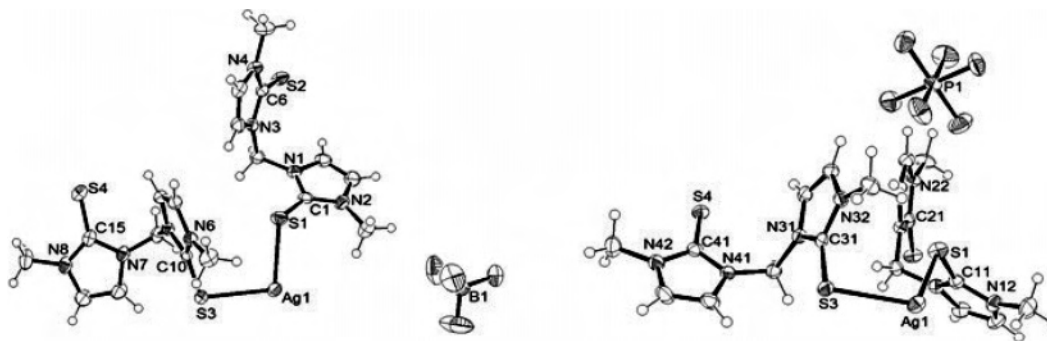


Figure 2. Asymmetric units of $\text{Ag}(\text{L1})_2(\text{X})$ [$\text{X} = \text{BF}_4$ (left) and PF_6 (right)]. Thermal ellipsoids are drawn at the 50% probability level.

The compound $[\text{Ag}_2(\text{L2})_2](\text{BF}_4)_2$ (**III**) crystallizes in the orthorhombic system. Systematic absences in the intensity data indicated the space groups $Pca2_1$ and $Pbcm$. $Pca2_1$ was eventually confirmed by the successful solution, refinement, and examination of the structure. This space group was further verified with PLATON/ADDSYM.¹³ The asymmetric unit contains one Ag_2 complex and two independent BF_4^- anions. One BF_4^- (B2–F8) is disordered over two orientations via rotation about the B2–F5 bond, in the ratio $A/B = 0.740(9)/0.260(9)$. The non-hydrogen atoms of the minor component of the disordered anion were refined with isotropic displacement parameters. The absolute structure (Flack) parameter of 0.21(2) indicates the data crystal is a partial inversion twin. The twinning was included in the final refinement cycles as described.¹²

The compound $[\text{Ag}_2(\text{L2})_2](\text{PF}_6)_2 \cdot 2\text{C}_3\text{H}_6\text{O}$ (**IV**) crystallizes in the triclinic system. The space group $P\bar{1}$ was assumed and confirmed by the successful solution and refinement of the structure. The asymmetric unit consists of one disilver complex, two acetone molecules of crystallization, and two hexafluorophosphate anions. One of the PF_6^- anions (P2/F7–F12) is disordered about two closely separated orientations in the refined ratio $P2A/P2B = 0.60(2)/0.40(2)$. The geometry of both disorder components was restrained to be similar to that of the ordered PF_6^- anion P1/F1–F6 (SHELX SAME instruction, 63 total restraints).

The compound $[\text{Ag}_4(\text{L2})_3](\text{PF}_6)_4 \cdot \text{CH}_3\text{CN}$ (**V**) crystallizes in the space group $P2_1/n$ as determined uniquely by the pattern of systematic absences in the intensity data. The asymmetric unit consists of one $\text{Ag}_4(\text{C}_9\text{H}_{12}\text{N}_4\text{S}_2)_3^{4+}$ complex, four independent PF_6^- anions, and a CH_3CN molecule of crystallization. One PF_6^- anion (P4, F19–F24) is disordered over two closely spaced positions with populations $A/B = 0.614(5)/0.386(5)$. Nearby counterpart atoms of each disorder component (e.g. P4A/P4B) were refined with identical displacement parameters. The geometry of the minor component was restrained to be similar to that of the major component (21 restraints).

The compound $[\text{Ag}_2(\text{L2})_2](\text{SO}_3\text{CF}_3)_2$ (**VI**) crystallizes in the space group $Pbca$ as determined uniquely by the pattern of systematic absences in the intensity data. The asymmetric unit contains one Ag_2 complex and two independent SO_3CF_3^- anions.

Results and Discussion

Synthesis. The reactions between $\text{CH}_2(\text{N-tim})_2$ (**L1**) and AgX ($\text{X} = \text{BF}_4$, PF_6 , OTf) in a 2:1 ligand:metal ratio in THF afforded the expected $\text{Ag}(\text{L1})_2\text{X}$ complexes in good yield. In the case of the triflate, it was also possible to isolate a 1:1 complex from the reaction between an equimolar ratio

of starting materials. Similar 1:1 complexes could not be isolated when either of the noncoordinating anions BF_4^- or PF_6^- were used; thus, it is likely that the triflate anion stabilizes such a 1:1 complex via its ability to coordinate metals through the oxygen atoms (vide infra).¹⁴ Support for this hypothesis is derived from the IR spectra of the solids which show characteristic S–O stretching bands for both uncoordinated (ca. 1280, 1032 cm^{-1})^{14a} and coordinated monodentate (ca. 1385, 1210, 980 cm^{-1})^{14b} triflate groups. It is fortunate that, in the case of $\text{Ag}(\text{L1})_2(\text{OTf})$ and $\text{Ag}(\text{L1})(\text{OTf})$, there are no (or only very weak) bands in this region (as determined by correlation with the spectra of the free ligand and of the silver tetrafluoroborate and hexafluorophosphate complexes).

Single crystals suitable for X-ray diffraction could only be obtained in the cases of $\text{Ag}(\text{L1})_2\text{X}$ ($\text{X} = \text{BF}_4$, PF_6). In these nearly isostructural complexes, the formation of coordination networks, as suggested from the ESI(+) mass spectra (vide infra), was verified. The structures of the asymmetric units clearly indicate the stoichiometry $\text{Ag}(\text{L1})_2\text{X}$ ($\text{X} = \text{BF}_4$, PF_6) and are given in Figure 2. These compounds form layered structures where the anions are sandwiched between cationic sheets. The cationic sheets are two-dimensional coordination networks constructed from divergent binding of ditopic ligands that bridge tetracoordinate silver centers. A view of this packing behavior in the hexafluorophosphate case is given in Figure 3, and packing views of the tetrafluoroborate analogue are provided in the Supporting Information. Within the coordination networks, the silver centers have distorted tetrahedral coordination geometries as a result of having four different silver–sulfur bond distances (2.55, 2.57, 2.61, and 2.63 Å in the case of tetrafluoroborate but 2.57, 2.58, 2.61, and 2.66 Å in the case of the hexafluorophosphate derivative). The average Ag–S bond distances in the AgBF_4 complex of 2.59 Å and in the AgPF_6 complex of 2.61 Å are in line with other known tetracoordinate silver compounds (vide infra).^{3d–f,4}

The NMR spectra of each of the three 2:1 complexes in acetone (slightly soluble) or CD_3CN (soluble) were relatively uninformative with regard to the solution structure as only a single set of resonances was observed shifted either up- or downfield from that of the free ligand (depending on the solvent), a typical situation for labile silver complexes. The

(13) Spek, A. L. *PLATON-A Multipurpose Crystallographic Tool*; Utrecht University: Utrecht, The Netherlands, 2003.

(14) (a) Lawrance, G. A. *Chem. Rev.* **1986**, *86*, 17. (b) Johnston, D. H.; Shriver, D. F. *Inorg. Chem.* **1993**, *32*, 1045.

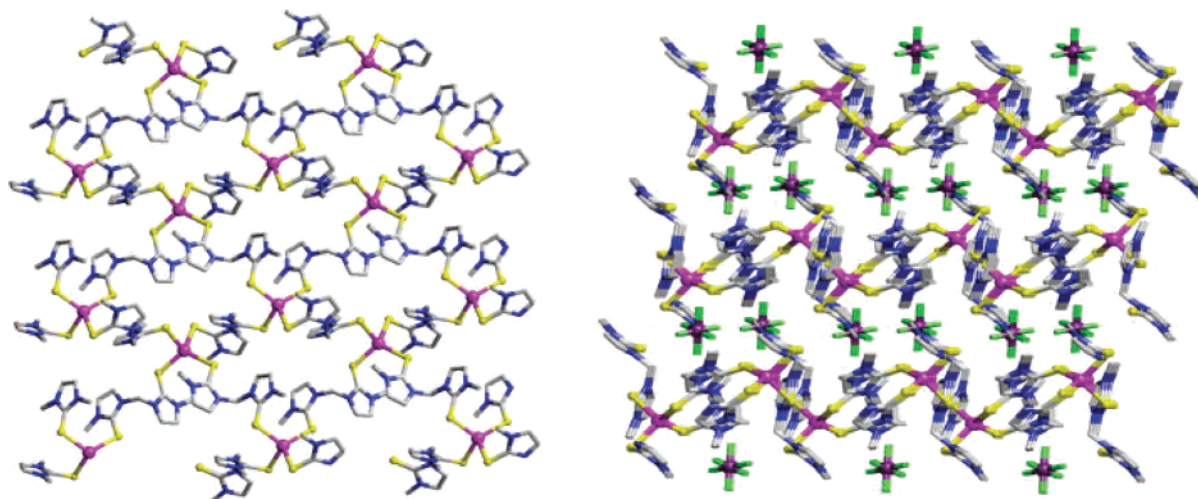


Figure 3. Left: Top view of the coordination network in $\text{Ag}(\text{L1})_2(\text{PF}_6)$ (anions removed for clarity). Right: Side view of the layered structure showing the sandwiching of PF_6^- anions.

same is true for the NMR spectrum of the pure 1:1 triflate complex which only has one set of ligand resonances but is not otherwise informative with regard to the true nature of this species in solution. It is possible to distinguish between the pure 2:1 and 1:1 triflate complexes in CD_3CN since the chemical shifts of imidazoline hydrogens in each case are significantly different. However, NMR spectra of mixtures of the two complexes in CD_3CN only show two imidazoline resonances, one methylene, and one *N*-methyl resonance at chemical shifts that are the weighted average of the chemical shifts found in the respective spectra of the individual components, indicating that ligand exchange occurs in CD_3CN , as expected.

The ESI(+) mass spectra of all the complexes in CH_3CN , which are thought to provide a more realistic (or at least more informative) sampling of the nature of the complexes in solution, showed numerous peaks with high *m/z* ratios consistent with the fragmentation patterns of silver-containing coordination polymers.¹⁵ This observation is highlighted by the results of the mass spectrum obtained for the hexafluorophosphate derivative, where peaks for cations containing Ag_4L_6 , Ag_4L_5 , Ag_3L_4 , Ag_3L_3 , Ag_2L_3 , Ag_2L_2 , AgL_2 , and AgL fragments (or their ion pairs; see Experimental Section) could be observed. The spectra of the tetrafluoroborate and the triflate derivatives were similar (with the appropriate substitution of anion in the ion pair peaks).

The electrochemistry of the complexes in CH_3CN with the corresponding NBu_4X , where X was either BF_4^- , PF_6^- , or OTf^- as the supporting electrolyte (Figure 4), was also indicative of metal complexation since an irreversible ligand oxidation [four-electrons from the $\text{Ag}(\text{L2})_2\text{X}$ stoichiometry] was found at ca. +0.9 V versus Ag/AgCl , a higher potential than +0.70 V for the free ligand under the same conditions. Moreover, there was an additional overlapping reversible wave, best detected by square-wave voltammetry, at ca. +1.1

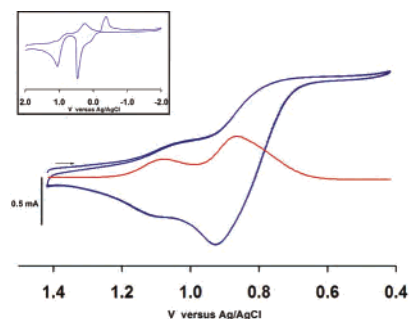


Figure 4. Cyclic and square wave voltammograms of $\text{Ag}(\text{L1})_2\text{BF}_4$ in CH_3CN with NBu_4BF_4 as the supporting electrolyte at a scan rate of 400 mV/s. The inset shows the highly irreversible waves associated with the Ag/Ag^+ couple. All other silver complexes show similar waves.

V versus Ag/AgCl that had about a quarter of the intensity (a one-electron oxidation) of the ligand oxidation wave. This reversible oxidation wave occurs close to that reported for the $\text{Ag}(\text{I})/\text{Ag}(\text{II})$ oxidation in another AgS_4 complex, the silver-thiacrown $[\text{Ag}([\text{15}]\text{aneS}_5)](\text{PF}_6)$,⁴ where electrochemically generated $\text{Ag}(\text{II})$ in this latter case was detected by ESR spectroscopy. The irreversible nature of the ligand oxidation in $\text{Ag}(\text{L2})_2\text{X}$ and presumably the high reactivity of oxidized species has thus far defied attempts to isolate and characterize any $\text{Ag}(\text{II})$ products. In addition to these oxidation waves, solutions of the complexes have highly irreversible waves at ca. +0.4 V (anodic) and -0.5 V (cathodic) that resemble those found for solutions of the “ligand-free” silver salts, corresponding to the $\text{Ag}^\circ/\text{Ag}^+$ couple.

The reactions between $\text{CH}_2(\text{S-tim})_2$ (**L2**) and AgX ($\text{X} = \text{BF}_4, \text{PF}_6, \text{OTf}$) in 1:1 ligand:metal ratios in THF afforded good yields of precipitates that had the expected empirical formula $\text{Ag}(\text{L2})\text{X}$ by elemental analyses. The crystal structures of all these derivatives revealed dimeric species where the ligands bridged two closely separated silver centers, as shown in Figure 5. In all three cases, the intracationic silver-silver distances (3.13 Å for $\text{X} = \text{BF}_4$, 2.98 Å for $\text{X} = \text{PF}_6$, and 3.14 Å for $\text{X} = \text{O}_3\text{SCF}_3$) are smaller than the sum of the van der Waals radii (3.40 Å) but are longer than the contact

(15) (a) Reger, D. L.; Wright, T. D.; Semeniuc, R. F.; Grattan, T. C.; Smith, M. D. *Inorg. Chem.* **2001**, *40*, 6212. (b) Reger, D. L.; Semeniuc, R. F.; Smith, M. D. *Eur. J. Inorg. Chem.* **2002**, 543. (c) Reger, D. L.; Semeniuc, R. F.; Smith, M. D. *Inorg. Chem. Commun.* **2002**, *5*, 278.

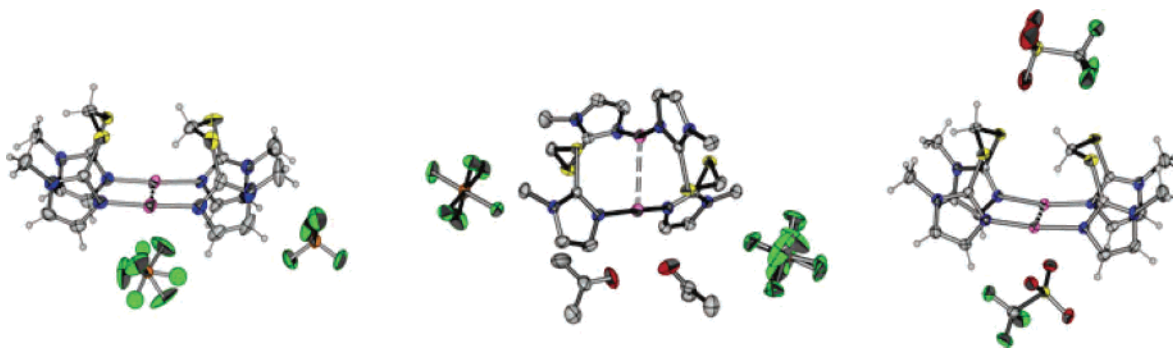


Figure 5. Asymmetric units in $\text{Ag}_2(\text{L}2)_2(\text{X})_2$ [$\text{X} = \text{BF}_4$ (left), PF_6 (middle, hydrogens removed, acetones of crystallization shown), OTf (right)].

radii in silver metal of 2.89 Å.^{16,22} The structures of the tetrafluoroborate and triflate derivatives share many features in common. In the BF_4 and OTf cases, where longer $\text{Ag}\cdots\text{Ag}$ contacts are found, the ligands are coincidentally disposed such that the heterocyclic rings on each ligand sit in an eclipsed, π -stacked manner constrained very close to one another. The average centroid–centroid distance for this intracationic heterocycle stacking is 3.41 Å in the case of the BF_4 and 3.56 Å in the triflate. These values are much shorter than the averages found for other π -stacked N-heterocycles such as 3.8 Å in the case of π -stacked pyridyls¹⁷ and 3.7 Å for π -stacked pyrazolyls.¹⁸ The eclipsed nature of the interaction is revealed in the small displacement angles β and γ that describe the slippage of two parallel displaced planes along the x and y directions (if z is the direction of interplanar stacking) where $\beta_{\text{avg}} = 13.8^\circ$, $\gamma_{\text{avg}} = 8.1^\circ$ for the tetrafluoroborate while $\beta_{\text{avg}} = 12.6^\circ$, $\gamma_{\text{avg}} = 4.7^\circ$ for the triflate. Slippage angles of around $\beta = 27^\circ$ are typically found in π -stacked pyridyl systems,¹⁷ which presumably represent the minimum energy (attractive) interaction of parallel displaced (offset) pyridyl rings. In a related case of the quadruple pyrazolyl embrace, attractive $\text{CH}-\pi$ interactions working in conjunction with $\pi-\pi$ interactions reduced the average slippage angle to $\beta = 16^\circ$, a value closer to that of an eclipsed system where $\beta = 0$. A perfectly eclipsed π -stacked geometry ($\beta = 0$) is expected to be repulsive owing to the direct overlap of electron-rich π -clouds. Thus, in the current cases, the repulsive nature of the short intracationic π -stacked interactions may be reflected in their interplanar dihedral tilting angles, α , which averages 11° in the BF_4 case and 16° in the triflate case; values between $\alpha = 2^\circ$ and 5° are found in about 95% of all other examples

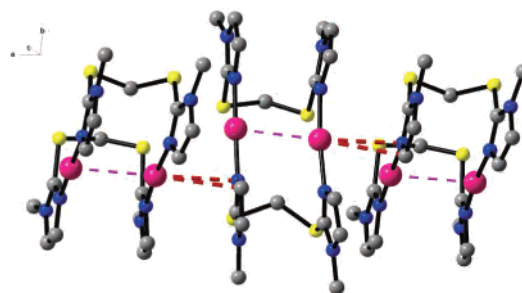


Figure 6. View of the stacking of dicationic units in $\text{Ag}_2(\text{L}2)_2(\text{BF}_4)_2$ along the a -direction as a result of $\text{Ag}-\pi$ interactions (red dashed lines). Short intracationic $\text{Ag}-\text{Ag}$ contacts are shown as pink-dashed lines.

of π -stacked N-heterocycles.^{17,18} Given the likely repulsive nature of stacking and potential Coulombic repulsions of the proximal cationic silver centers, it might be surprising that these structures would be formed in the first place. However, a closer inspection of the packing structure of these complexes reveals the presence of a possible additional stabilizing interaction. In $\text{Ag}_2(\text{L}2)_2(\text{X})_2$ ($\text{X} = \text{BF}_4$, OTf), the electron densities of the thioimidazoline π -systems (and the electron deficient nature of the silver cations) may be reduced by the presence of a cation– π interaction.¹⁹ This interaction occurs between the imidazoline ring fragment of one dication and $\text{Ag}(2)$ of a neighboring dication such that the dicationic units assemble into chains that propagate along the a -axis (Figure 6). One consequence of this stacking is that the silver centers appear to be aligned into a wirelike fashion throughout the crystal; however, the intercationic $\text{Ag}\cdots\text{Ag}$ separations are much longer than twice the van der Waals radii of silver, so any intercationic metallophilic interaction is unlikely. An additional consequence of the cation π -interaction could be a reduction in the slip angle β from the typical value of $\beta = 27^\circ$ to the observed values near $\beta = 13^\circ$, in a similar way that the $\text{CH}-\pi$ interaction stabilized a smaller β value in the “quadruple pyrazolyl embrace”. The three-dimensional packing of these two compounds $\text{Ag}_2(\text{L}2)_2(\text{X})_2$ ($\text{X} = \text{BF}_4$, OTf), completed as a result of other weak noncovalent interactions ($\text{CH}-\pi$, $\text{CH}-\text{F}$, $\text{CH}-\text{O}$, and $\text{Ag}-\text{O}$, as summarized in the Supporting Information), may also serve to support the unusual structural arrangement of the dication motifs.

The structure of the PF_6^- salt is strikingly different than its tetrafluoroborate and triflate counterparts. First of all, the former crystallizes as an acetone solvate whereas the latter two crystallized free of solvent. Moreover, the hexafluoro-

- (16) Bondi, A. *J. Phys. Chem.* **1964**, *68*, 441.
 (17) Janiak, C. *J. Chem. Soc., Dalton Trans.* **2000**, 3885.
 (18) Reger, D. L.; Gardinier, J. R.; Semeniuc, R. F.; Smith, M. D. *Dalton Trans.* **2003**, 1712.
 (19) (a) Ma, N. L. *Chem. Phys. Lett.* **1998**, *297*, 230. (b) Klippenstein, S. I.; Dunbar, R. C. *J. Phys. Chem. A* **1997**, *101*, 3338. (c) Lindeman, S. V.; Rathore, R.; Kochi, J. K. *Inorg. Chem.* **2000**, *39*, 5707. (d) Munakata, M.; Wu, L. P.; Ning, G. L.; Kuroda-Sowa, T.; Maekawa, M.; Suenaga, Y.; Maeno, N. *J. Am. Chem. Soc.* **1999**, *121*, 4968. (e) Munakata, M.; Wu, L. P.; Sugimoto, K.; Kuroda-Sowa, T.; Maekawa, M.; Suenaga, Y.; Maeno, N.; Fujita, M. *Inorg. Chem.* **1999**, *38*, 5674.
 (20) (a) Reger, D. L.; Gardinier, J. R.; Smith, M. D. *Inorg. Chem.* **2004**, *43*, 3825. (b) Reger, D. L.; Watson, R. P.; Gardinier, J. R.; Smith, M. D. *Inorg. Chem.* **2004**, *43*, 6609. (c) Chen, C.-L.; Tan, H.-Y.; Yao, J.-H.; Wan, Y.-Q.; Su, C.-Y. *Inorg. Chem.* **2005**, *44*, 8510.
 (21) Shannon, R. D. *Acta Crystallogr.* **1976**, *A32*, 751.
 (22) Pykkö, P. *Chem. Rev.* **1997**, *97*, 597.

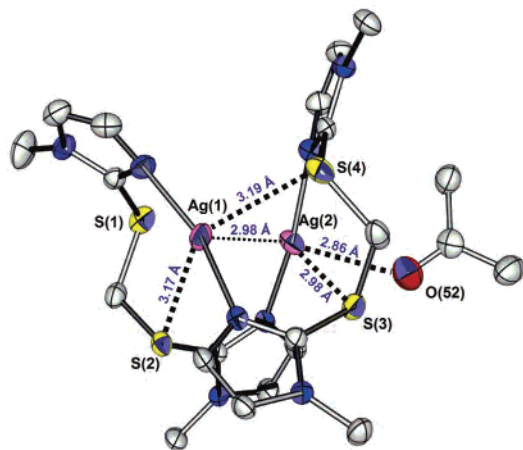


Figure 7. Dication in $\text{Ag}_2(\text{L}2)_2(\text{PF}_6)_2 \cdot 2\text{acetone}$ showing bonding (solid lines) and secondary interactions (thicker dashed lines) of the central $\text{Ag} \cdots \text{Ag}$ unit (pink). (Hydrogens and the second, noninteracting, acetone of crystallization were removed for clarity.)

phosphate salt has the shortest internuclear $\text{Ag} \cdots \text{Ag}$ distance of the three derivatives at 2.98 Å (which is much shorter than the sum of the *covalent* radii of silver of 3.18 Å). The silver centers are bonded to the nitrogen atoms of the ligand at an average distance of 2.133 Å which is slightly longer than $\text{Ag}-\text{N}_{\text{avg}} = 2.098$ Å found in the BF_4 case and than $\text{Ag}-\text{N}_{\text{avg}} = 2.109$ Å in the triflate but is in line with other known silver complexes with nitrogen donors.^{18,20} The ligands in the dimeric $\text{Ag}_2(\text{L}2)_2(\text{PF}_6)_2$ structure each bridge two silvers (as in the previous cases) and are very distorted precluding any repulsive intraligand $\pi-\pi$ stacked eclipsed geometry. In fact, the ligand distortion is such that a bridging, bidentate N,N,S mode (rather than a simple N,N-bridging mode) *might* (incorrectly) be inferred from an examination of the coordination spheres of silver. A detailed view of the structure of the dication showing primary bonding and weak secondary interactions can be found in Figure 7. There are

multiple close silver–sulfur contacts between 2.62 and 4.19 Å which are the sums of the covalent and van der Waals radii of the atoms, respectively. However, determining whether any of these actually constitute some sort of “bonding” interactions by simply inspecting Ag–S distances is, at best, difficult since a cursory literature search showed a wide range of Ag–S distances (2.3–3.2 Å) that are claimed to be due to bonding interactions.

In an attempt to clarify the matter of ambiguous silver–sulfur “bond” distances, two Cambridge Structural Database searches of compounds containing at least one Ag–S bond were performed, and those compounds which were not polymeric, had no errors, and had R-factors of less than 0.075 were included in both searches. In a more exclusive search, an attempt was made to avoid ambiguity regarding the silver coordination spheres by omitting those results that had a silver–metal bond in the coordination sphere. The resulting search yielded 268 data sets with 1104 occurrences because there is often more than one Ag–S bond/data set. In the more inclusive search, those that indicated metal–metal bonds were included, and this search yielded 342 data sets with 1408 occurrences. The data from this larger set showed the same trend as found in the more exclusive search; however, there was a much broader distribution (and a greater uncertainty) of distances in the compounds with higher coordination numbers. The broad distribution Ag–S distances in the larger search set likely reflects the greater uncertainty in what constitutes either a silver–metal or a silver–sulfur bonding interaction; the cavalier assignment of either obviously affects the coordination number. This greater uncertainty is reflected in the fact that in the full search there are several instances of “seven-coordinate” silver while in the exclusive search there are none. Full details of the inclusive search can be found in the Supporting Information. Perhaps in accord with the apparent increase in ionic

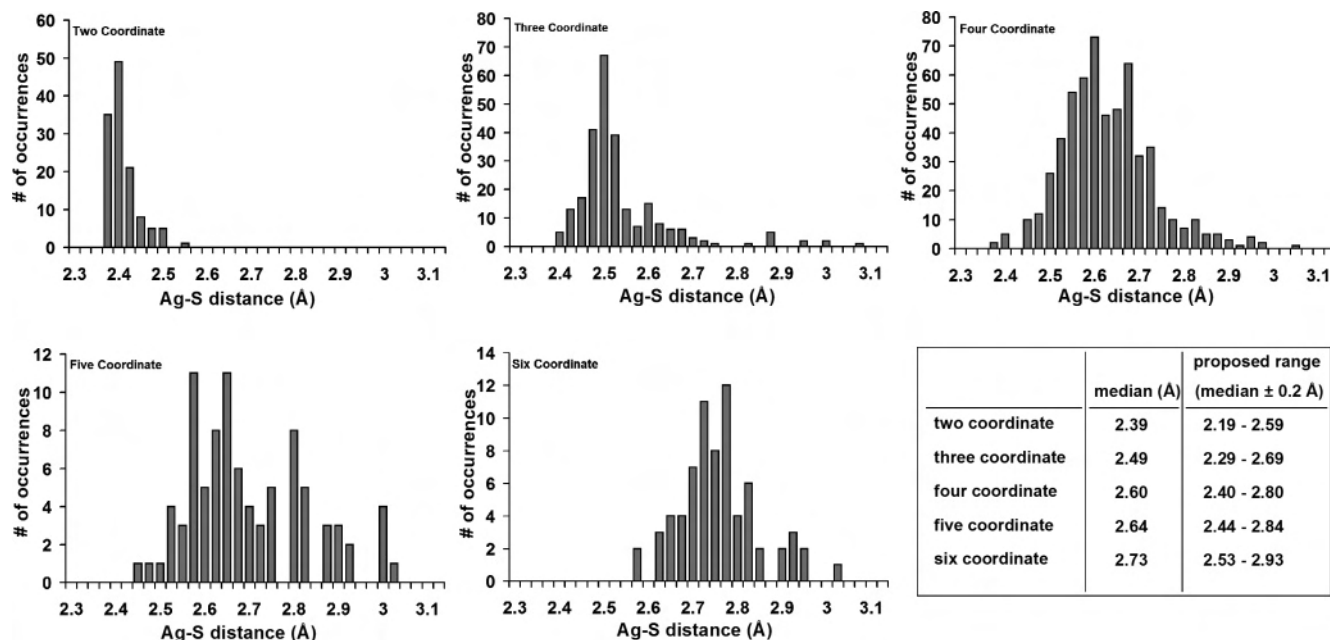


Figure 8. Histograms of number of occurrences versus Ag–S bond distances obtained from the Cambridge Structural Database search for (a) two-, (b) three-, (c) four-, (d) five-, and (e) six-coordinate complexes with at least one Ag–S bond.

radii of silver with increasing coordination number [0.81 Å (two coordinate), 1.14 Å (four coordinate), 1.29 Å (six coordinate), etc.],²¹ the silver–sulfur bond distances depend highly on the metal’s coordination number. The results of the more exclusive database search are summarized in Figure 8. For two-coordinate silver, Ag–S bonds averaged 2.40 Å but ranged from 2.36 to 2.53 Å. Three-coordinate silver had an Ag–S bond-distance average of 2.52 Å but a range of 2.39–3.00 Å. Four-coordinate silver had an average Ag–S distance of 2.62 Å but a range of 2.36–3.04 Å. The average distances and the ranges for five- and six-coordinate silver were similar at 2.70 Å (2.48–3.01 Å) and 2.75 Å (2.57–3.00 Å), respectively. The broad distribution of Ag–S bond distances in the data sets for higher coordination numbers reflects what was reported in the original literature and is likely a little too disperse since alternative (better) descriptions of coordination geometries/number, at least in the case of pentacoordination, probably existed for the compounds with Ag–S distances at the extremes of the scale. Regardless, from the above data, one could propose that reasonable bond distances would include those that range from the median distance to ± 0.2 Å (Figure 8, bottom right); such a proposal would minimize contributions from the likely errors in assignment of coordination geometries at the extremes (especially for higher coordination numbers). For instance, silver–sulfur internuclear separations ranging from 2.6 to 3.0 Å would be the reasonable lower and upper limits for “bonding interactions” for *six-coordinate* silver.

In the case of $\text{Ag}_2(\mathbf{L}2)_2(\text{PF}_6)_2 \cdot 2\text{acetone}$, if one were not to consider the short silver...silver contact as being part of the coordination sphere, then both silvers would be two-coordinate. However, given that the silvers are closer than the sum of the covalent radii, it may be better to consider each metal atom as part of the coordination sphere of the other. Thus, along with the data extracted from the above search, both silvers are best described as three-coordinate with Ag(1)N₂Ag(2) kernels in distorted T-shaped geometries. While it might be tempting to assign a higher coordination number to Ag(2), the relatively long silver–sulfur internuclear separations [the shortest being Ag(2)–S(3) at 2.98 Å] are outside the proposed reasonable range for both tetracoordinate silver and (along with the long silver–oxygen distance) even for the alternative description of a five-coordinate AgN_2SO distorted trigonal bipyramidal geometry. These long Ag–S and Ag–O contacts outside the primary “covalent” bonding sphere of silver, which also happen to be much less than the sum of the respective van der Waals radii of the elements, might best be classified as secondary interactions, a likely result of electrostatic/ion-dipole attractions. A possible consequence of these secondary interactions is the observed ligand distortion possibly facilitated by the presence of acetone. The overall effect may be a reduction of effective charge density on the metal centers in the silver hexafluorophosphate case, allowing the silvers to come into closer proximity compared to the BF_4 and triflate cases. In all three complexes of this ligand, the anions participate in weak $\text{CH}\cdots\text{X}$ ($\text{X} = \text{O}, \text{F}$, as appropriate) interactions that

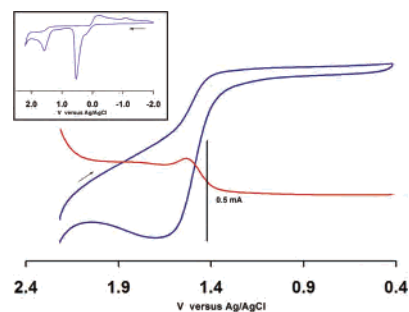


Figure 9. Cyclic (400 mV/s) and square wave voltammograms of $[\text{Ag}_2(\mathbf{L}2)_2](\text{BF}_4)_2$ in CH_3CN with NBu_4BF_4 as the supporting electrolyte. The inset shows a scan in the reverse direction highlighting the highly irreversible waves associated with the Ag/Ag^+ couple. The forward and reverse scans of all nitrogen-bonded $[\text{Ag}_2(\mathbf{L}2)_2](\text{X})_2$ ($\text{X} = \text{BF}_4, \text{PF}_6, \text{OTf}$) complexes are similar.

complete the three-dimensional packing arrangements; these might also influence the observed $\text{Ag}\cdots\text{Ag}$ distances in the solid state.

The NMR spectra of each of the three $\text{Ag}_2(\mathbf{L}2)_2(\text{X})_2$ complexes in either acetone or CD_3CN show only one set of resonances that are shifted either up- or downfield from the free ligands. Thus, like the linkage isomers described above, the NMR spectral data permit the detection of ligand complexation and indicate rapid exchange is occurring (especially since AB multiplets might be expected for the methylene hydrogen resonances if the solid state structures were maintained in solution), but they do not otherwise reveal the nature of the complexes in solution. The IR spectra of the triflate derivative both in solution and in the solid show only S–O stretches for the uncoordinated ion (1280, 1030 cm^{-1}), indicating that the close proximity of one of the two triflates observed in the solid state structure (Supporting Information) is probably the result of electrostatic (pure Coulombic or ion–dipole) attractions instead of having any significant covalent bonding character. The bands near 520 cm^{-1} are indicative of the weak $\text{CH}\cdots\text{F}$ interactions observed in the solid-state structures.²³ The ESI(+) mass spectra of the three derivatives in CH_3CN show the expected signals for the $\text{Ag}_2(\mathbf{L}2)_2$ moiety as the ion pairs, $[\text{Ag}_2(\mathbf{L}2)_2(\text{X})]^+$, where X is BF_4^- , PF_6^- , or OTf^- , in addition to the fragmentation peaks $[\text{Ag}(\mathbf{L}2)_2]^+$, $[\text{Ag}(\mathbf{L}2)]^+$ (monomer), and solvated $[\text{Ag}(\text{CH}_3\text{CN})_2]^+$. Unfortunately, unlike other compounds with short $\text{Ag}\cdots\text{Ag}$ contacts,²⁴ none of the current complexes are luminescent in solution or in the solid state.

Interestingly, the cyclic and square wave voltammograms of these complexes (Figure 9) show only one irreversible two-electron ligand oxidation at ca. +1.5 V versus Ag/AgCl , a higher potential than for the first oxidation of the free ligand (ca. +1.2 V) under the same conditions. In these nitrogen-bonded silver derivatives, additional highly irreversible, history-dependent waves at about +0.5 and –0.3 V versus Ag/AgCl corresponding to the Ag^0/Ag^+ couple are observed;

(23) Reger, D. L.; Semeniuc, R. F.; Rassolov, V.; Smith, M. D. *Inorg. Chem.* **2004**, *43*, 537.

(24) (a) Rawashdeh-Omary, M. A.; Omary, M. A.; Patterson, H. H.; Fackler, J. P., Jr. *J. Am. Chem. Soc.* **2001**, *123*, 11237. (b) Rawashdeh-Omary, M. A.; Omary, M. A.; Patterson, H. H. *J. Am. Chem. Soc.* **2000**, *122*, 10371.

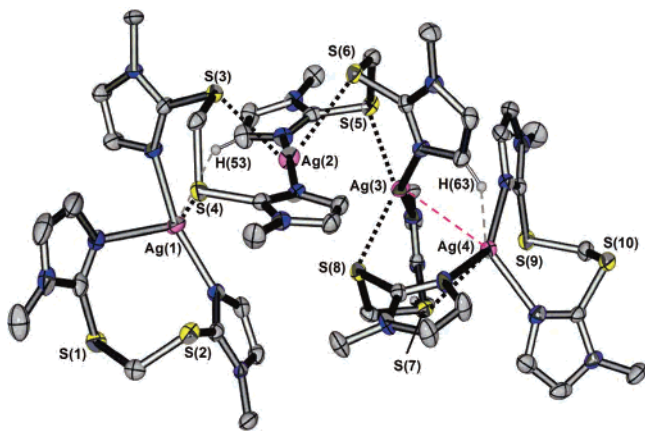


Figure 10. Structure of cation in $\text{Ag}_4(\text{L}2)_5(\text{PF}_6)_4$ with 50% probability ellipsoids and where most hydrogens have been removed for clarity. All of the short contacts to silver are shown. The $\text{Ag}\cdots\text{S}$ interactions $< 3.15 \text{ \AA}$ are given by thick dashed lines. The short $\text{Ag}\cdots\text{Ag}$ contact (3.06 \AA) is shown by the thin dashed (pink) line, and “short” $\text{Ag}\cdots\text{H}$ contacts $< 4.0 \text{ \AA}$ are shown by thin gray dashed lines.

as before, these are only slightly different from those found for the “ligand-free” silver salts. In none of the three cases were waves for an $\text{Ag}^{\text{I}}/\text{Ag}^{\text{II}}$ couple detected. The shift in ligand oxidation to higher potential is in accord with the expected increased difficulty in oxidation of a positively charged complex compared to the charge-neutral ligands. However, the change in number of observed oxidation waves is noteworthy. Since the cyclic voltammograms of all three complexes are similar (but the solid state structures clearly differ), the change in number of oxidation waves likely indicates that there is no longer electronic communication between π -stacked rings as found in the charge neutral/monocationic free ligand system. Thus, the π -stacked geometry observed in the solid state of the tetrafluoroborate and triflate cases no longer exists in solution, as might be anticipated if the π -stacked geometry were repulsive as described above. Alternatively, the second oxidation wave may be outside the potential window of this experiment. This scenario, while feasible, might be less likely given the similarity in the voltammograms of the three complexes (with different solid-state structures) and because a dicationic ligand is not expected to be capable of effectively coordinating a silver(I) cation.

Inspired by the results of the ESI(+) mass spectra for the above three complexes, we decided to pursue whether it would be possible to isolate a tetracoordinate bis(chelate) compound of the type $\text{Ag}(\text{L}2)_2\text{X}$ (for which we arbitrarily chose the hexafluorophosphate) by using the appropriate ligand:metal ratio in the preparative reaction; however, the desired species was never isolated. Instead, reactions between $\text{CH}_2(\text{S-tim})_2$ and AgPF_6 afford $\text{Ag}_4(\text{L}2)_5(\text{PF}_6)_4 \cdot \text{solvent}$ as the only silver-containing product when the ligand:metal ratio is equal to or greater than 1.5. Using lower ligand:metal ratios from 1 to 1.33 (including 5:4!) resulted only in the isolation of $\text{Ag}_2(\text{L}2)_2(\text{PF}_6)_2$. The structure of the cation in $\text{Ag}_4(\text{L}2)_5(\text{PF}_6)_4 \cdot (\text{CH}_3\text{CN})$ is given in Figure 10. In this remarkable structure, four silver atoms are connected into a chain by bridging ligands. The internuclear separation between $\text{Ag}(3)$ and $\text{Ag}(4)$ of 3.06 \AA is noteworthy in that it is shorter

than twice the *covalent* radii of silver, while the other two silver–silver distances are relatively long at 3.71 and 3.58 \AA for $\text{Ag}(1)–\text{Ag}(2)$ and $\text{Ag}(2)–\text{Ag}(3)$, respectively. If one were to consider the short $\text{Ag}(3)\cdots\text{Ag}(4)$ contact to represent some sort of weak “bonding interaction”,²² then the coordination geometries for $\text{Ag}(1)–\text{Ag}(4)$ are distorted T-shaped, linear, distorted square planar, and distorted tetrahedral, respectively. In this scenario, $\text{Ag}(1)$ has a nearly planar AgN_3 kernel ($\sum_{\text{N}–\text{Ag}–\text{N}} \text{angles} = 356.7^\circ$), where the alternative description of a distorted tetrahedral AgN_3S is less likely since the $\text{Ag}–\text{S}$ distance of 2.86 \AA is outside the reasonable range for tetracoordinate silver and the resulting tetrahedron would be extraordinarily distorted from ideal geometry. The $\text{Ag}(1)–\text{S}(2)$ distance of 3.59 \AA and $\text{Ag}\cdots\text{H}$ distance of 3.45 \AA are far too long to consider a pentacoordinate geometry. Similar arguments can be used to support that $\text{Ag}(2)$ with long $\text{Ag}(2)–\text{S}$ distances of 2.88 and 2.99 \AA (outside the range for tetracoordinate silver) has a nearly linear $[\text{N}(41)–\text{Ag}–\text{N}(51) = 170.4^\circ]$ AgN_2 kernel rather than a very distorted tetrahedral AgN_2S_2 geometry. On the other hand, the $\text{Ag}–\text{S}$ bond distances $\text{Ag}(3)–\text{S}(3)$ of 2.69 \AA and $\text{Ag}(3)–\text{S}(6)$ of 2.73 \AA fall within the range found for pentacoordinate silver. Therefore, the $\text{AgN}_2\text{S}_2\text{Ag}(4)$ kernel can best be described as a distorted square pyramidal arrangement as indicated by the τ parameter $\tau = 0.21$, where $\tau = 0$ represents an ideal square pyramid and $\tau = 1.0$ represents an ideal trigonal bipyramid.²⁵ Finally, $\text{Ag}(4)$ is best described as tetracoordinate with a $\text{Ag}(4)\text{N}_3\text{Ag}(3)$ kernel arranged in a distorted tetrahedron. The closest silver–sulfur contact $\text{Ag}(4)–\text{S}(7)$ of 3.02 \AA is outside the proposed reasonable range for pentacoordinate silver. In this description of the cation structure, the close $\text{Ag}–\text{S}$ contacts that fall just outside the proposed “covalent bonding” range but that are well below the sum of the van der Waals radii of the respective elements would be considered secondary interactions. The sulfur donor atoms are then oriented toward silver as a result of attractive electrostatic ion–dipole forces.

The NMR, IR, electrochemical data, and ESI(+) mass spectra of this species in acetonitrile differ only minutely from those of $\text{Ag}_2(\text{L}2)_2(\text{PF}_6)_2$, indicating rapid ligand exchange in solution, as in the above cases. The differences are only slight shifts in the respective spectra and that high mass species can be detected *in the baseline* of the ESI(+) mass spectrum in the current case. It is likely, given the forcing conditions needed for the preparation of this compound and the similar spectral properties this compound shares with $[\text{Ag}_2(\text{L}2)_2](\text{PF}_6)_2$, that this species dissociates in solution to give the more stable dimeric species and free ligand in accord with the following equilibrium:



In fact, attempts to recrystallize analytically pure samples of this unusual complex (from CH_3CN and Et_2O) always afford a nearly equal mixture of prismatic $[\text{Ag}_4(\text{L}2)_5](\text{PF}_6)_4 \cdot \text{CH}_3\text{CN}$ and fibrous $[\text{Ag}_2(\text{L}2)_2](\text{PF}_6)_2$. We are cur-

(25) Addison, A. W.; Rao, T. N.; Reedijk, J.; van Rijn, J.; Verschoor, G. C. *J. Chem. Soc., Dalton Trans.* **1984**, 1349.

rently pursuing the nature of the proposed equilibrium with this and other silver salts in order to determine whether any other oligomeric members of this class of “metal–organic ring-opening polymerization” fragments can be isolated.

Summary and Conclusions. The two symmetric linkage isomers of the $\text{CH}_2(\text{tim})_2$ compounds are versatile, electroactive ligands for coordination chemistry. In the case of $\text{CH}_2(\text{N-tim})_2$, previous studies have demonstrated both a chelating mode and a bridging mode of coordination depending on the metal system.⁷ A bridging mode of coordination was identified in the current chemistry with silver salts. With silver tetrafluoroborate and hexafluorophosphate, $[\text{Ag}(\text{L2})_2(\text{X})]_n$ complexes are formed that have the anions sandwiched between cationic layers where bridging sulfur-donating ligands span tetracoordinate silver centers forming two-dimensional coordination networks. When the anion is triflate, both $[\text{Ag}(\text{L2})_2(\text{OTf})]_n$ and $[\text{Ag}(\text{L2})(\text{OTf})]_n$ of unknown structures are formed; however, in each, both monodentate and noncoordinated triflates are detected by IR spectroscopy. All of these sulfur-bound silver complexes appear to remain complexed in solution as evidenced by the NMR spectra and since the electrochemical data show a shift in ligand oxidation to more positive potentials. The electrochemical data also suggest that it may be possible to access the unusual Ag(II) oxidation state using these ligands, and this goal is currently being pursued by our laboratories.

The compound $\text{CH}_2(\text{S-tim})_2$ is an even more versatile ligand than its CN_2 linkage isomer since simple chelating, simple bridging, and the newly identified dual bridging/chelating mode of metal-binding are found in its silver complexes. When ligands are combined with silver salts in ligand:metal ratios from 0.5 up to about 1.4, cyclic dimeric products with simple bridging ligand binding modes are obtained. With larger excess of starting ligand (a ratio of 1.5 and higher), an unusual $\text{Ag}_4(\text{L2})_5(\text{PF}_6)_4$ compound was isolated, where the ligands exhibited all three of the above-mentioned binding modes. The dual chelating/bridging binding mode was identified with the help of a Cambridge

Structural Database search that was performed to determine what constitutes a reasonable silver–sulfur “covalent” bonding interaction. From the results of the search, it was found that silver–sulfur bond distances can reasonably range from about 2.2 to 3.0 Å, where the average distances increase with increasing coordination number. Silver–sulfur internuclear distances in cationic complexes that extend beyond about 3.0 Å but that are smaller than about 4 Å are likely brought into close proximity as a result of ion–dipole interactions rather than by any covalent interactions. The structures of all four of these nitrogen-bound silver complexes in solution, like most other silver complexes, remain uncertain. The combined NMR, electrochemical, and mass spectral data indicate both ligand complexation and exchange, but it is still unknown to what extent, if any, ligand dissociation occurs or whether the peaks identified in the ESI(+) spectra of acetonitrile solutions of the complexes are due solely to fragmentation during the ionization process (or whether these fragments are actually present in solution prior to electrospray ionization). Regardless, these ligand exchange/dissociation processes are likely responsible for the solvent- and anion-dependent crystallization behaviors in silver coordination chemistry. Furthermore, by introduction of a sulfur heteroatom along the ligand backbone, it was possible to access an unusual tetrameric chain structure stabilized via the multiple covalent bonding modes of the ligand and this structure is probably further supported by intracationic electrostatic ion–dipole interactions.

Acknowledgment. We thank Bill Cotham and Mike Walla (University of South Carolina) for obtaining the mass spectral data. J. R. G. thanks Marquette University and the Petroleum Research Fund for support.

Supporting Information Available: Additional figures and discussion regarding supramolecular structures and crystallographic information files (CIF). This material is available free of charge via the Internet at <http://pubs.acs.org>.

IC052025A